

Accepted Manuscript

A comparison of thermal comfort conditions in four urban spaces by means of measurements and modelling techniques

Juan A. Acero, Karmele Herranz-Pascual



PII: S0360-1323(15)30042-1

DOI: [10.1016/j.buildenv.2015.06.028](https://doi.org/10.1016/j.buildenv.2015.06.028)

Reference: BAE 4172

To appear in: *Building and Environment*

Received Date: 14 April 2015

Revised Date: 24 June 2015

Accepted Date: 26 June 2015

Please cite this article as: Acero JA, Herranz-Pascual K, A comparison of thermal comfort conditions in four urban spaces by means of measurements and modelling techniques, *Building and Environment* (2015), doi: 10.1016/j.buildenv.2015.06.028.

This is a PDF file of an unedited manuscript that has been accepted for publication. As a service to our customers we are providing this early version of the manuscript. The manuscript will undergo copyediting, typesetting, and review of the resulting proof before it is published in its final form. Please note that during the production process errors may be discovered which could affect the content, and all legal disclaimers that apply to the journal pertain.

**A comparison of thermal comfort conditions in four urban spaces by means of
measurements and modelling techniques**

Juan A. Acero*, Karmele Herranz-Pascual

TECNALIA, Energy and Environmental Division, Parque Tecnológico de Bizkaia, Edificio700, 48160

Derio, Bizkaia, Spain,

*Corresponding autor: juanangel.acero@tecnalia.com, Tel. +34 946 430 850, Fax: +34 901 760 009

Abstract

Microclimatic conditions inside urban areas depend on the result of the interaction of the regional climate with the whole urban area and on the local characteristics of the urban development. Inadequate human thermal comfort conditions can affect quality of life and the use of public open spaces. In this study, outdoor thermal conditions are examined through three field campaigns in Bilbao in the north of the Iberian Peninsula. Climate variables are measured in four different areas of the city in different regional climate conditions. Thermal comfort evaluation is undertaken by means of the thermal index PET (Physiological Equivalent Temperature). Measurements are compared with estimated values derived from ENVI-met model. Results show that the differences between modelled and measured climatic variables can imply a relevant deviation in PET (i.e. difference between modelled and measured values). Regression and correlation analyses account for the importance of the deviation of each climatic variable in the deviation of PET values. Deviation of PET appears to be highly conditioned by the deviation of mean radiant temperature values especially during clear sky days. Under overcast conditions deviation of wind speed also becomes a relevant aspect. Consequently, reliable estimation of these variables is required if modelling techniques are to be used in the assessment of thermal comfort in outdoor urban spaces.

1. Introduction

Inside urban areas the alteration of the radiation budget and the wind pattern is responsible for significant spatial variations of thermal comfort. Thus, urban microclimatic conditions do not only vary from those of rural areas, but also present important changes in short distances (e.g. direct sun radiation exposure versus shadow sites). Local thermal comfort is influenced by the location and orientation of buildings and other urban elements like vegetation [1,2], the materials used [3,4] and of course the interaction of the whole urban area with the regional climate [5].

In a context of climate change and with the aim of improving quality of life and health inside the urban areas [6,7], urban planners are considering more and more the thermal component of climate in order to develop comfortable urban areas [8]. In this sense, collaboration with urban climate experts to develop human bioclimatological studies turns to be essential [9,10].

Adequate design of outdoor urban spaces (e.g. urban squares) not only conditions thermal comfort levels but also the use pedestrians do of it [11]. Assessment of thermal comfort requires the use of methods and indices which combine meteorological variables with thermophysiological parameters [12,13]. Human biometeorological indices have been developed to describe thermal stress [14]. One of them is the well-known Physiological Equivalent Temperature (PET) Index [15,16]. Four climatic variables are required for thermal comfort assessment: air temperature, wind speed, mean radiant temperature and relative humidity. These can be undertaken by means of micrometeorological measurements [17–19] and/or modelling [20–23]. However, models do not always derive precise results due to limitations of spatial resolution and the approaches to account for the ambient conditions (i.e. dynamic and radiative aspects).

ENVI-met [24,25], RayMan [26] or Solweig [27] are well known models used to evaluate thermal comfort. However, their approaches are different. While ENVI-met is based on computational fluid dynamics (CFD) and thermodynamics, RayMan and SOLWEIG are basically 3D radiation models. In the context of urban design ENVI-met has been extensively used due to its capability to combine and consider spatial variations of the 4 climatic variables influencing thermal comfort [18,21,28,29].

Using the new ENVI-met model (v 4.0), the aim of this study is to quantify the differences between modelled and measured thermal comfort conditions in four outdoor urban spaces with

different development and in different meteorological conditions. The study applies regression and correlation analyses to evaluate deviation of PET values. Additionally, the model performance is evaluated using different quantitative difference metrics that analyse the accuracy of the simulations. Based on the results, identification of modelling limitations is established.

2. Description of ENVI-met model

The ENVI-met model is a three-dimensional non-hydrostatic microclimate model developed to calculate and simulate climate variables in urban areas with a typical grid resolution of 0.5 to 10 meters. The model considers a complete radiation budget (i.e. direct, reflected and diffused solar radiation and longwave radiation). It models the evolution of climate variables during diurnal cycles using laws of fluid dynamics and thermodynamics. The ENVI-met model calculates the state of the atmosphere by combining the influence of buildings, vegetation, surfaces characteristics, soils and climatic contour conditions [24].

ENVI-met has been used and tested intensively for different aims specially the effects of different urban design options on outdoor thermal environment [2,20,28,30]. However, most of these studies used older versions of ENVI-met (v 3.0/3.1).

The new version of ENVI-met (v4.0) includes significant modifications to previous versions. The principal is the possibility to force climate variables along the simulation to account for atmospheric temporal variations and consequently represent better the evolution of meteorological variables along the day. Also, together with the previous 1D vegetation module (i.e. plants are modelled as vegetation columns), the new version implements a new 3D vegetation module to describe varied shapes of plants and spatial distribution of the leaves. Finally, the building module in version 4 also accounts for the heat inertia of wall and roof [25,31,32].

The main input parameters for ENVI-met include meteorological data, initial soil wetness and temperature profiles, structure and properties of ground surfaces, vegetation elements and buildings. 1D boundary model (from the ground level to 2500 m height) is used for the initialization of the model and for the boundary model conditions of the 3D atmospheric model. The 3D model area include the different elements (e.g. buildings), and is where the main ENVI-met variables are calculated (wind speed and direction; air and soil temperature; air and soil humidity; turbulence; radiative fluxes and gas and particle dispersion). Thus, updating the 1D boundary meteorological conditions (e.g. each hour) as in ENVI-met v4.0 is expected to show

better performance than v3.1 when evaluating thermal comfort conditions along the diurnal cycle.

However, ENVI-met (v4.0) has several limitations. It is important to note that only air temperature and relative humidity boundary conditions are updated along the diurnal simulation. Thus, wind speed and direction as well as cloudiness remains constant. Additionally, the model can neither simulate precipitation nor temperatures below the freezing point. As described in Huttner [31] ENVI-met is based on Reynolds Averaged Navier-Stokes (RANS) equations with a 1.5 order turbulence closure model which tends to overestimate the turbulent production k in areas with a high acceleration or deceleration, such as the flow around a building and thus, influencing wind speed estimation. Finally, the calculation of radiation fluxes is not accurate [31].

3. Methodology

3.1 Study areas

Considering Bilbao land use classification [33] and the regional climate affecting the urban area (see section 3.2), four urban areas with different local climate were selected inside the city. Their location can be seen on Fig. 1. *Ribera* is an urban park located in an open-set area beside the river waterway (i.e. the most important ventilation path that crosses through the middle of the urban area); *Miribilla* is a boulevard in an open-set highrise urban development in one of the most elevated areas of the city; *Casco Viejo* is a square in the old part of city with a very dense urban development (i.e. compact lowrise); and *Indautxu* is also a square in a compact midrise district in the city centre (Fig. 2).

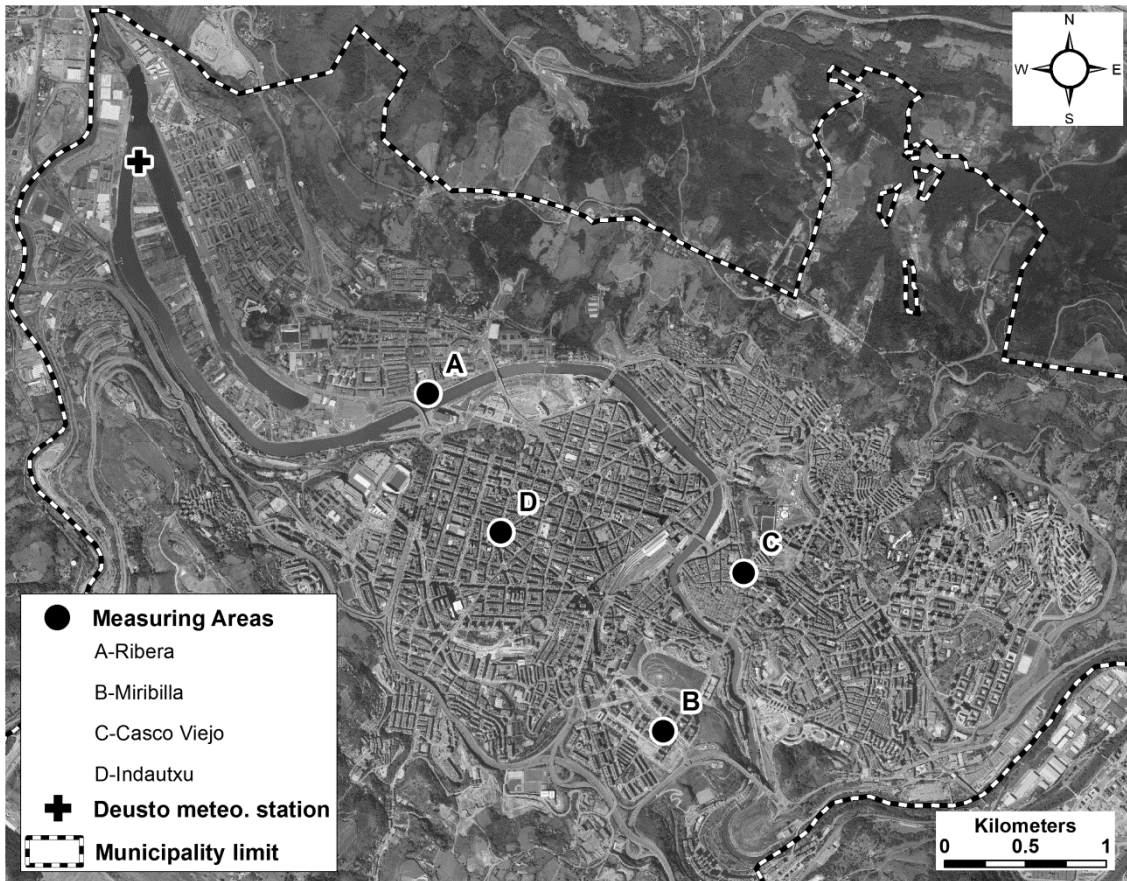


Fig. 1 Location of the measuring areas during the campaigns in Bilbao. Location of *Deusto* meteorological station (Basque Meteorological Agency)

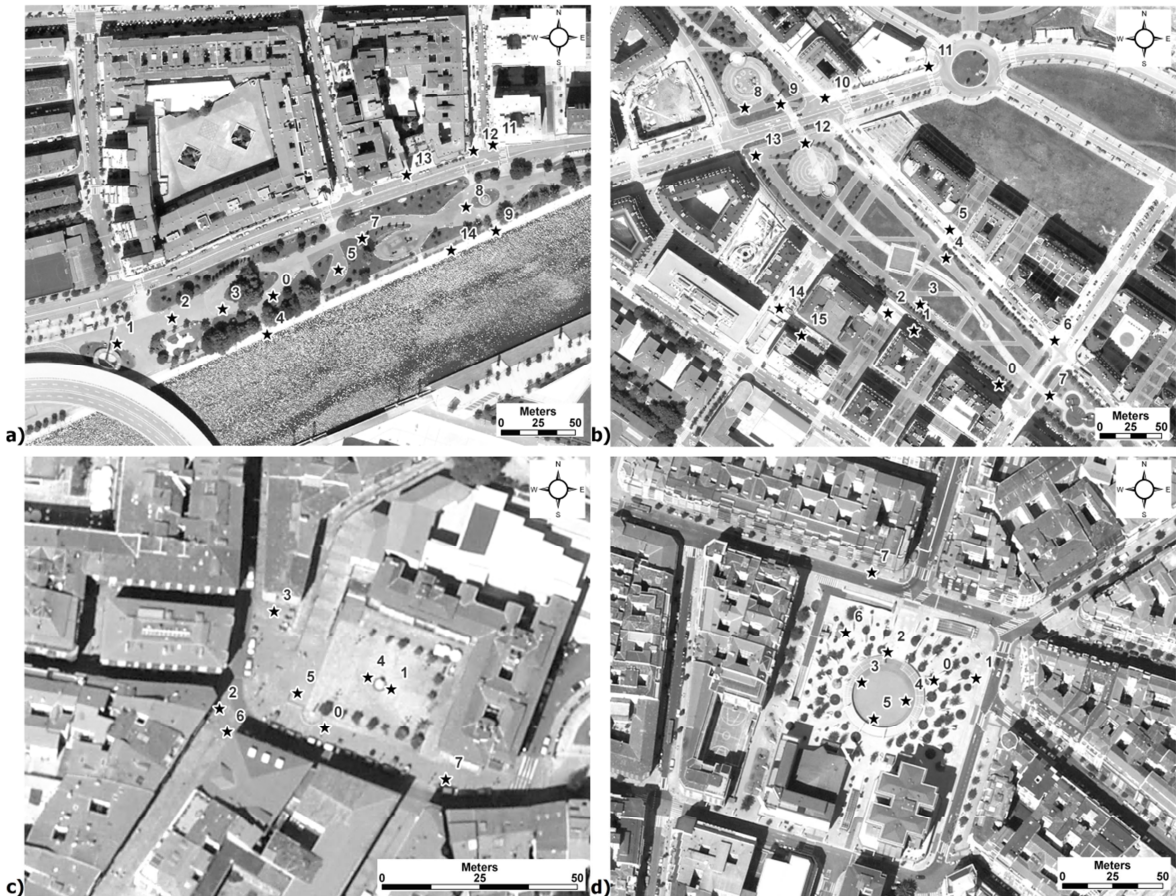


Fig. 2 Measurement sites (stars) inside the areas of a) *Ribera* b) *Miribilla* c) *Casco Viejo* and d) *Indautxu*

3.2 Regional climate

Bilbao is located in the northern part of the Iberian Peninsula. The main urban area is densely built-up ($21,200 \text{ inhabitants}/\text{km}^2$) with not much open spaces. River Nervión flows through the middle of the urban area and is one of the most important ventilation paths of the city.

The regional climate in Bilbao is characterized by moderate temperatures in winter and summer influenced by the proximity of the Atlantic Ocean. Annual mean temperature is $14-15^\circ\text{C}$. Summer season does not usually register high temperatures. Daily maximum temperature (T_{\max}) is highest in July and August (i.e. $T_{\max} 26.2^\circ\text{C}$ and 25.5°C respectively). However, heat waves can occur several times per year during summer and air temperature can reach up to 40°C [34].

Relative humidity is quite constant during the year. Mean monthly values at summer are around 70-72%. Typical precipitation is in the range of 1,100-2,000 mm/year. Rain is more frequent in spring and autumn while July is the month with less rain. Cloudy skies are frequent. Approximately 50% of the time cloud cover is greater than 6 oktas [35].

Atmospheric dynamics is influenced in an important way by complex terrain and sea/land interactions [36]. Surface air flow usually adapts to the topography and air masses are channelled through the valley. Both topography and proximity of the sea are factors that develop sea/land and mountain/valley breezes which occur with relatively high frequency especially in stable atmosphere situations.

Distance to the seashore and topography orientation influence local ventilation potential and thus local climate inside Bilbao urban area. Consequently, despite the whole region is influenced by the same regional climatic phenomena, specific areas inside Bilbao present different climate characteristics [33].

3.3 Measurement campaigns

The measurement campaigns consisted in recording climatic variables inside the selected areas with mobile devices. Specific measuring sites inside each area were selected to provide relevant and representative climate data of the area (Fig. 2).

Measurements were carried out during three days (6th to 8th August 2010) with typical summertime weather (i.e. influence of sea breeze) from sunrise to sunset covering all the sunlight hours. Each day, measurements were carried out in two areas. Mobile sensors were moved from one site to another during the campaigns. The period in each measuring site (i.e. >15 minutes) was appropriate to record representative data and evaluate the micrometeorological conditions.

All the climatic instruments were installed in an easy moving shopping cart (Fig. 3). The following variables were measured: air temperature (Ta), relative humidity (RH), wind speed (WS), wind direction (WD) and globe temperature (Tg). Data of the first four variables were obtained with a unique device: the Weather Transmitter WXT520 of Vaisala. Tg measurements were carried out using a 40-mm table tennis ball (i.e. a hollow acrylic sphere) painted with grey color (RAL 7038) with a PT100 temperature sensor inside the middle of the ball. This method for Tg calculation has been tested and has shown to be effective in outdoor conditions [37,38]. The measuring system recorded 1 minute average values at 1.1 meter a.g.l. The sensors provided the following accuracy for the measurements: $\pm 0.3^{\circ}\text{C}$ for Ta and Tg, $\pm 3\%$ for RH, and $\pm 3\%$ for WS and WD. Mean radiant temperature (Tmrt) was derived from the previous measurements following the equation [37]:

$$T_{mrt} = \left[\left(T_g + 273.15 \right)^4 + \frac{1.335 \times 10^8 WS^{0.71}}{\varepsilon D^{0.4}} \times \left(T_g - T_a \right) \right]^{\frac{1}{4}} - 273.15$$

where T_g is the globe temperature ($^{\circ}\text{C}$), WS is the wind speed (ms^{-1}), T_a is the air temperature ($^{\circ}\text{C}$), D is the globe diameter (m) and ε is the globe emissivity. In our case $\varepsilon = 0.95$.

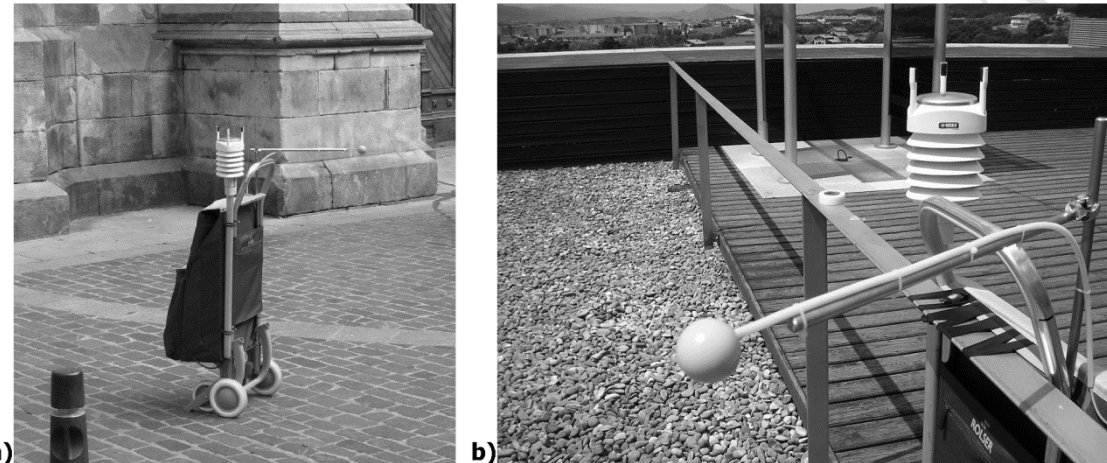


Fig. 3 Mobile measuring system developed for Bilbao campaigns. The devices installed were: Vaisala WXT520 and globe temperature device

Additionally, 10-minute average data of WS , RH , Ta and total incoming radiation measured in *Deusto* (station from the Basque Meteorological Network) were used to evaluate regional meteorological conditions affecting Bilbao urban area during the measurement campaigns. This site is located in an open area surrounded by water and exposed directly to the unperturbed sea breeze front reaching the urban area prior to be influenced by the urban heat island (Fig. 1).

3.4 Model configuration

In this study, ENVI-met version 4 [25] is used forcing the model with real Ta and RH occurring along the day. The rest of the meteorological conditions remain constant along the simulation (e.g. wind speed and solar radiation).

Considering the period of the measurements (i.e. from sunrise to sunset), simulations were launched at 4:00 local time (i.e. UTC+2), approximately 3 hours before sunrise. The background air flow characteristics that forced the model were taken from *Deusto* meteorological station. The total modelling time was 20 hours which included the period when measurements were carried out. Discrete receptors were defined in the model for the locations of the measurements. For these, output meteorological data were available every 10 minutes.

Characteristics of the model domain in each area are presented on Table 1. The vertical definition of all the model domains considered a 0.4 m vertical grid size in the 5 lowest grid cells. The size of the rest of the vertical grid cells was defined as increasing with height (except in *Casco Viejo*) due to the presence of high buildings and the model maximum vertical grid cells limitation. The horizontal grid resolution was defined in correspondence with the width of the streets. Specific vegetation elements were defined in the model to account for the properties of vegetation species in the modelled areas. The trees height ranged from 4 to 15 meters, leaf area density ranged from 0.8 to 2.15 m²/m³ and the albedo was 0.2 for all the species. Definition of trees considered the presence of leaves only in the crown. However, an accurate representation of the crown form was not possible because the 1D vegetation module of ENVI-met was used (i.e. vegetation are represented as candlesticks).

Table 1 Description of the model dimensions of each area

Model parameter	Area			
	Ribera	Miribilla	CascoViejo	Indautxu
Number of grid cells (x,y,z)	167, 104, 30	167, 146, 30	109, 101, 26	167, 167, 30
Size of grid cells (meters) (x,y,z)	2, 2, increasing with height	2, 2, increasing with height	1.5, 1.5, 2	2, 2, increasing with height
Nesting grids	6	6	9	6
Soil profiles in nesting grids	Deepwater & Pavement	Loamy & Pavement	Asphalt & Pavement	Asphalt & Pavement
Model rotation out of grid north	-19°	39°	18°	16.6°

The meteorological boundary conditions used by the model were extracted from data registered on *Deusto* meteorological station except for cloud cover and specific humidity at 2500 m. Cloud cover information was obtained from Bilbao airport station [10] and specific humidity at 2500 m was obtained from US-NCEP (United States National Centers for Environmental Prediction) Reanalysis data. Hourly evolution of Ta and RH (i.e. data used to force the model), and WS and WD are shown on Fig. 4. Since WS and WD temporal variations during the simulations period could not be considered by the model, each day the median value of the hourly data between 10:00 and 20:00 (UTC) was used as input. Each day between these hours air flow characteristics registered in *Deusto* were quite similar and corresponded to a well-established sea breeze. Thus, WS and WD model results were only expected to be reliable during this regional condition. Since ENVI-met requires WS at 10 m a.g.l., data measured at *Deusto* (i.e. 30 m a.g.l.) were adjusted using the power law for wind profile [39]:

$$WS_{10} = WS_h(10/h)^{\alpha}$$

where WS_h is the wind speed (ms^{-1}) at the height of h and α is an empirical exponent which depends on the surface roughness. In our case $\alpha = 1/7$ because the measurements were done in an open terrain with obstacles not closer than 75 meters.

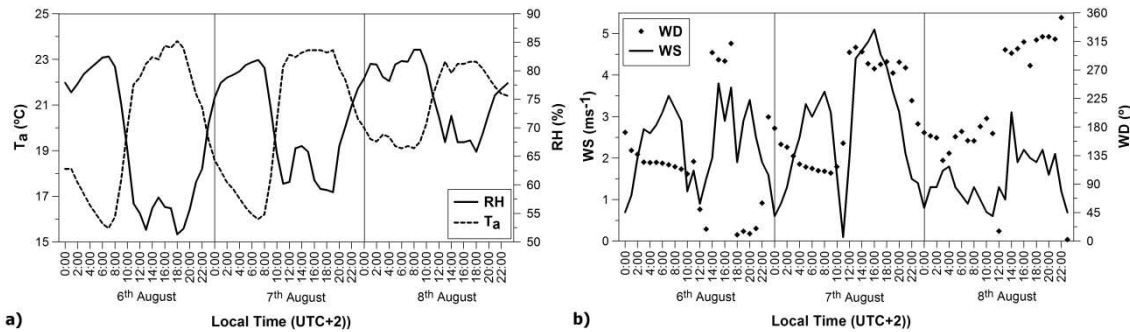
Similarly to WS and WD, a constant cloud cover value for all the simulation was selected despite differences occurred along the day (Table 2). Data input to the model were registered at 13h (UTC). Model estimation of solar radiation was adjusted by comparing direct and diffuse shortwave radiation estimations in the absence of building with the total incoming radiation in *Deusto* station. The solar factor selected to adjust the shortwave solar radiation calculated by the model for each simulation period (i.e. each day) was at 12.00 (UTC). Due to lack of information of soil moisture and temperature initial conditions, model default values were used. The meteorological input parameters are shown in Table 3.

Table 2 Cloud cover records at Bilbao airport station.

Day	Hour	Cloud cover (octans)
6th August	7	7
	13	5
	18	0
7th August	7	0
	13	1
	18	1
8th August	7	8
	13	8
	18	8

Table 3 Description of the model meteorological boundary configuration of each area

Meteorological variable	Day		
	6th August	7th August	8th August
Wind Speed at 10 m a.g.l.	2.31 m/s	3.69 m/s	1.67 m/s
Wind direction	292°	281°	314°
Roughness length	0.2	0.2	0.2
Cloud cover (octans)	5	1	8
Specific humidity (2500 m)	3.5 g/kg	4.5 g/kg	6 g/kg
Solar adjust Factor	0.86	0.86	1.37
Soil upper layer (0-20 cm) initial temperature			
Soil middle layer (20-50 cm) initial temperature			Default by model: 293 K
Soil deep layer (>50 cm) initial temperature			
Soil upper layer (0-20 cm) moisture content			Default by model: 50 %
Soil middle layer (20-50 cm) moisture content			Default by model: 60%
Soil deep layer (>50 cm) moisture content			

**Fig. 4** Measured meteorological conditions in *Deusto* station. Hourly evolution of a) air temperature (Ta) and relative humidity (RH), and b) wind speed (WS) and wind direction (WD)

3.5 Model evaluation

The model performance was done by comparing the measured data with ENVI-met results of Ta, vapour pressure (e), WS and Tmrt. PET [40] was used to assess the model reliability of thermal comfort levels.

At each site, with the aim of obtaining representative measured data, 10-minute mean values were calculated [37]. However, the first 10-minute mean Tmrt value at each site was not reliable due to the time the sensor required to adapt to the new site. This was noticed specially when moving from sun exposed to shadow sites and vice versa. So, during the first 10 minutes, mean Tmrt was calculated with the last minute value of the 10-minute period since this value was reliable. For the following 10 minutes at the same site, mean Tmrt was calculated with the 1-

minute Tmrt values. In the case of Ta, *e* and WS, 10-minute mean values were always calculated with 1 minute values.

To evaluate the model performance at each site, every 10-minute mean measurement of Ta, *e*, WS and Tmrt was compared with the temporally closest modelled data (i.e. every 10 minutes). Comparison was made with ENVI-met output values at 1 meter height.

To assess thermal comfort by means of PET, Ta and RH (or *e*) conditions as well as radiation and wind data (i.e. Tmrt and WS) are required. Previously calculated 10-minute of measured and modelled values were used. Additionally, the human metabolic heat rate and other personal parameters need to be considered (e.g. age, gender, clothing, weight and height). For this study, PET was calculated with standardized data (i.e. age: 35 years, height: 1.75; metabolic rate: 80w/m²; clothing: 0.9; weight: 75 kg; sex: man).

Correlation analyses were performed to evaluate the relationship between modelled and measured climate variables.

Finally, seven regression analyses were performed to identify the importance of the deviation (i.e. modelled – measured) of each climate variable in Δ PET (i.e. PET_{modelled} - PET_{fieldstudy}; where PET_{modelled} is obtained from the modelling and PET_{fieldstudy} is obtained from the measured climate variables in the field campaigns). Δ PET was considered as the dependent variable while the independent variables were Δ Tmrt, Δ WS, Δ T and Δ RH. In the stepwise regression, variables can be entered or removed depending on the model significance (probability) of the F-value or the eigenvalue of F. The first regression analysis included all the data available (i.e. 335 sets of data), while the other six were performed for each day and in each area where the measurements were carried out (Table 4).

Table 4 Number (N) of measured and modelled pairs for each area and selected day

Day	Area			
	<i>Ribera</i>	<i>Miribilla</i>	<i>Casco Viejo</i>	<i>Indautxu</i>
6 th August	N=65	N=54		
7 th August			N=62	N=66
8 th August		N=23	N=65	

4. Results and discussion

4.1 Comparison of measured & modelled climate variables

The results of the comparison of modelled and measured climate variables depend on:

1. The regional meteorological conditions during each day of campaign and,
2. The urban development type of each area and its location inside the whole city

Following, a synthesis of the analysis for each variable is presented:

Temperature and air humidity

The best relationship between modelled and measured data is for Ta (Table 5). Low Pearson correlation coefficients for e in *Ribera* and *Miribilla* are attributed to their different location and local characteristics with respect to the site from where the data that force the model are taken (i.e. *Deusto*). In the case of *Ribera*, the high presence of greenery increases evapotranspiration and thus air humidity. On the other hand, *Miribilla* is affected by cold air drainage winds during the morning [33] and thus has different air properties.

Table 5 Correlation between measured and modelled wind speed (WS), air temperature (Ta), vapour pressure (e) and mean radiant temperature (Tmrt) for each area and selected day, as well as for all data available.

		Tmrt	Ta	WS	e
6 th August	<i>Ribera</i>	0.76**	0.97**	0.03 ⁽¹⁾	0.33 ⁽¹⁾
	<i>Miribilla</i>	0.86**	0.97**	-0.15 ⁽¹⁾	0.01 ⁽¹⁾
7 th August	<i>Indautxu</i>	0.64**	0.98**	-0.06 ⁽¹⁾	0.86**
	<i>CascoViejo</i>	0.73**	0.99**	0.15 ⁽¹⁾	0.84**
8 th August	<i>Miribilla</i>	0.64**	0.96**	-0.64**	0.40 ⁽¹⁾
	<i>CascoViejo</i>	0.63**	0.97**	0.01 ⁽¹⁾	0.61**
All days and areas		0.70**	0.92**	0.32**	0.90**

** p<0.001

(1) = no significance

Differences between pairs of modelled and measured Ta (Table 6) are more relevant in the two compact areas, *Indautxu* and *CascoViejo*, during the clear sky day (7th August) when mean ΔTa ($\text{Ta}_{\text{modelled}} - \text{Ta}_{\text{measured}}$) is -1.4°C and -1.6°C respectively. In the case of *Indautxu* highest $\|\Delta\text{Ta}\|$ values occur around midday (Fig. 5). Afterwards, during the afternoon, $\|\Delta\text{Ta}\|$ tends to reduce. Results are in correspondence with the urban heat island effect (i.e. accumulated heat). This phenomenon is noticed in the measured values since the modelling results are forced by Ta from *Deusto* (suburban area) where the urban heat island effect is negligible [33]. On the other hand results for Δe ($e_{\text{modelled}} - e_{\text{measured}}$) show that during the afternoon e_{measured} tends to increase with respect to e_{modelled} (Fig. 5) in relation to the establishment of a well-developed sea breeze after midday that incorporates easily humidity into the urban area (e.g. *Indautxu*). The increase of e inside the urban area due to the presence of sea breezes was demonstrated in Acero et al. [33].

Table 6 Mean differences between modelled and measured wind speed (WS), air temperature (Ta), vapour pressure (e) and mean radiant temperature (Tmrt) for each area and selected day

	6 th August				7 th August				8 th August			
Area	Δ WS (m/s)	Δ Ta (°C)	Δ e (hPa)	Δ Tmrt (°C)	Δ WS (m/s)	Δ T (°C)	Δ e (hPa)	Δ Tmrt (°C)	Δ WS (m/s)	Δ Ta (°C)	Δ e (hPa)	Δ Tmrt (°C)
Ribera	0.6	-0.7	-0.3	3.4								
Miribilla	0.6	0.5	-0.2	5.7					0.8	-0.1	0.7	1.6
Indautxu					1.5	-1.4	-1.0	17.4				
Casco Viejo					-0.5	-1.6	-0.1	5.7	-0.4	-0.9	-0.2	-7.7

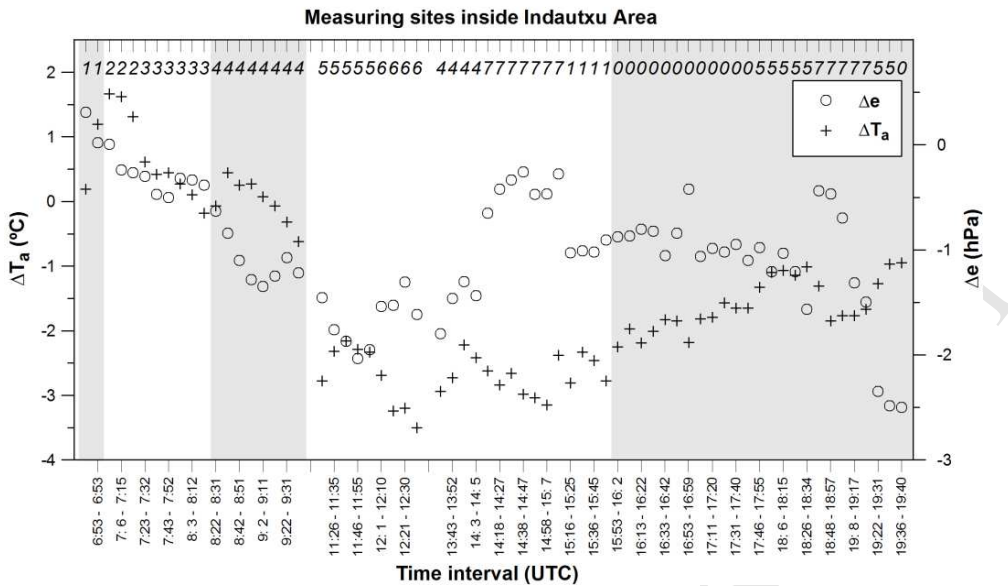


Fig. 5 ΔT_a ($T_{a\text{modelled}} - T_{a\text{measured}}$) and Δe ($e_{\text{modelled}} - e_{\text{measured}}$) temporal evolution in *Indautxu*. Darkened areas represent non-direct sun exposed periods. The rest represent direct sun exposed periods

The proximity of the river waterway is well noticed in *Ribera*. The waterway in the city of Bilbao is considered an important ventilation path that can provide cold and humid air to the urban area [33]. In *Ribera*, the results show that during daytime $T_{a\text{measured}}$ is always higher than $T_{a\text{modelled}}$ (i.e. $\Delta T_a < 0$) except during the first hours after sunrise (i.e. until 9:00 UTC). This morning drift occurs when solar radiation heats up urban surface but water temperature remains cold. Thus, T_a forcing the model (from *Deusto* station surrounded by water) is colder than the measurements. Highest $|\Delta T_a|$ occur in sites 12 and 13 after midday reaching -2.9°C (Fig. 6). This result is in agreement with the location of these sites and the period of the day when they were recorded. Sites 12 and 13 are the closest locations (3-4 meter) to a south oriented building façade and are the farthest from the river waterway (Fig. 2). Consequently, the cooling effect of the water surface [41,42] and of the sea breeze is reduced. During the afternoon, sites influenced by the shadow of big dense trees present $\Delta T_a \sim 0^{\circ}\text{C}$ (i.e., site 0) caused by a reduction in $T_{a\text{measured}}$. These vegetation elements are also responsible for $\Delta e < 0$ especially in the late afternoon under building shadow conditions. During this period the effect of evapotranspiration of dense trees in the park becomes more relevant. Results are consistent with the capability of urban greenery to reduce T_a during daytime [2,22,43] as well as increase air humidity inside urban areas [44,45].

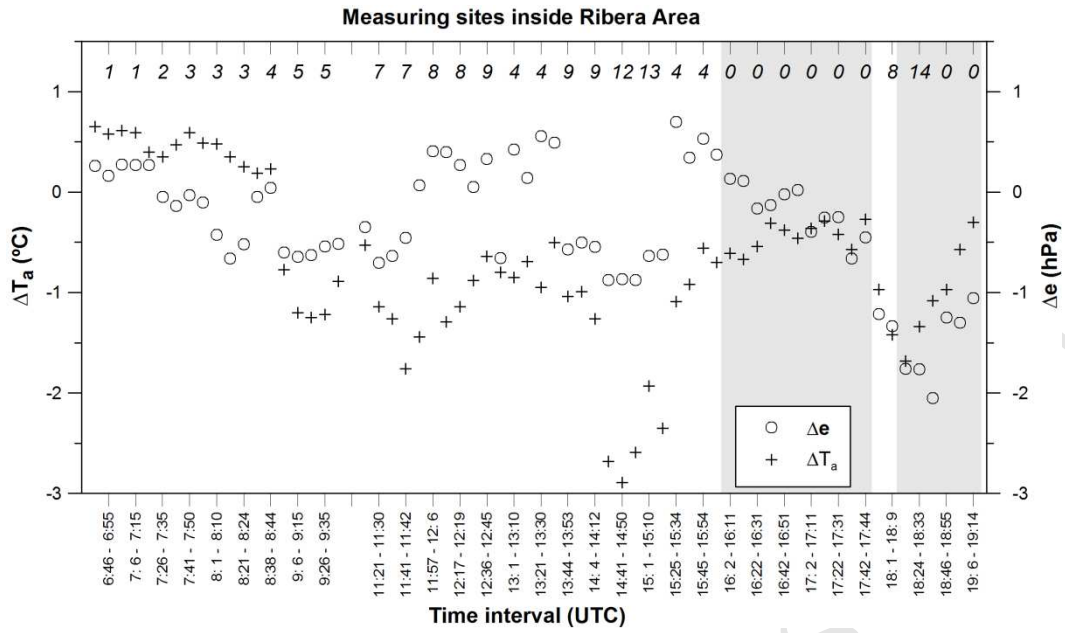


Fig. 6 ΔT_a ($T_{a\text{modelled}} - T_{a\text{measured}}$) and Δe ($e_{\text{modelled}} - e_{\text{measured}}$) temporal evolution in *Ribera*.

Darkened areas represent non-direct sun exposed periods. The rest represent direct sun exposed periods

In the case of *Miribilla*, its elevated location on a hillside conditions the characteristics and evolution of ΔT_a along the day. On 6th August (a partly covered day) ΔT_a reaches +2.1°C during the morning (Fig. 7). Before midday all ΔT_a values are positive (i.e. $T_{\text{modelled}} > T_{\text{measured}}$) while during the afternoon ΔT_a are mostly negative which is in accordance with the influence of cold downslope winds during the morning hours previous to the sea breeze influence. In the same way Δe tends to increase from negative values in the morning to $\Delta e > 0$ around midday. Afterwards, during the afternoon, with relevant influence of the sea breeze in *Miribilla* measured and modelled Ta and e values present little differences showing that urban heat accumulation in *Miribilla* is minimized by the cooling effect of regional sea breeze. The effect of this meteorological phenomenon in other areas of the city is different [10] and should be taken into consideration during the urban planning processes due to its influence in Bilbao's climate [33]. Other urban areas around the world are also affected in a similar way by this urban ventilation phenomenon [46,47].

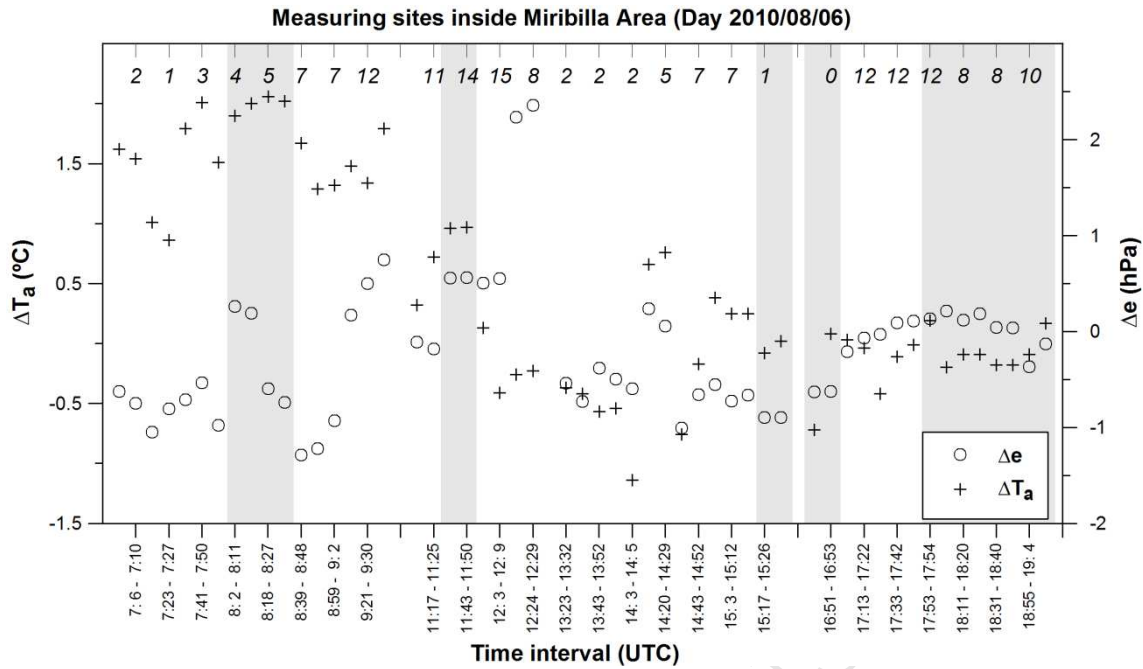


Fig. 7 ΔT_a ($T_{a\text{modelled}} - T_{a\text{measured}}$) and Δe ($e_{\text{modelled}} - e_{\text{measured}}$) temporal evolution in *Miribilla*. Darkened areas represent non-direct sun exposed periods. The rest represent direct sun exposed periods

Wind Speed

Modelled WS values do not represent correctly measured data. This result is justified because the model is driven by an initial WS and WD which does not change during the simulation period and obviously differs from the temporal variation of the regional air flow direction in Bilbao (Fig. 4). WS_{modelled} is slightly underestimated in *Casco Viejo* independently of the regional meteorological condition, while in *Indautxu* it is highly overestimated (Table 6). Results are in accordance with comments presented in Huttner [31] and other studies showing limitations of ENVI-met to provide accurate estimations of wind speed [48] especially if wind speed is greater than 2 m/s [30].

Mean Radiant Temperature

T_{mrt} does not show good relationship between measured and modelled values (Table 5), mainly because of two reasons. On one hand, the model tends to overestimate shortwave radiation ($S_{w, \text{modelled}}$) during all daytime except midday in correspondence with the adjustment of solar radiation with measured data at 12:00 UTC. Thus $T_{mrt, \text{modelled}}$ is expected to present higher values than the ones measured during the morning and afternoon periods. On the other hand, model resolution does not differentiate precisely shadowing caused by certain urban elements which results in significant deviation between modelled and measured T_{mrt} .

The significant overestimation of direct $S_{w, \text{modelled}}$ radiation during the morning and afternoon periods is well represented in *CascoViejo* during the clear sky day (7th August) (Fig. 8). This is the main reason for $T_{mrt, \text{modelled}}$ overestimation (e.g. ΔT_{mrt} ($T_{mrt, \text{modelled}} - T_{mrt, \text{measured}}$)) in site 2 during the morning $\sim +24^\circ\text{C}$). At midday, when modelled solar radiation is adjusted to measurements, locations exposed directly to solar radiation present $\Delta T_{mrt} \sim +7^\circ\text{C}$ (i.e. site 5) while under building shadow conditions, $\Delta T_{mrt} \sim +5^\circ\text{C}$ (i.e. site 6). Results are consistent with the urban geometry characteristics at each site since diffuse S_w radiation is reduced with lower sky view factor (case of site 6). These results (i.e. $\Delta T_{mrt} \neq 0$) show that not only direct $S_{w, \text{modelled}}$ radiation is overestimated during the morning and afternoon but that there are errors in other radiation components (e.g. diffuse/reflected $S_{w, \text{modelled}}$ radiation, longwave ($L_{w, \text{modelled}}$) radiation) which could be caused by an incorrect model evaluation of the surface albedos and temperature, and vegetation properties (e.g. leaf area index) which finally derives in an incorrect estimation of T_{mrt} . Overestimation of direct $S_{w, \text{modelled}}$ has also been reported by other authors using ENVI-met [18,22]. In any case, the calculation of the whole radiation fluxes described in Huttner [31] as not accurate, can justify the deviation of $T_{mrt, \text{modelled}}$.

Imprecise definition of buildings (i.e. height) and the resolution of the vertical grid also causes an unreal estimation of direct solar radiation exposure with significant consequences in ΔT_{mrt} . This can clearly be noticed during the clear sky day (7th August) in *CascoViejo* on sites 3&4 before midday and site 0 during the afternoon (Fig. 8) when $\Delta T_{mrt} < 0$ (between -15 and -20°C). In this case the model expects the sites to be under shadow conditions but the measurements were really done under direct solar radiation despite the shadow from the building was close to the sensor (as noted during the field campaign).

The absence of direct solar radiation during the overcast day (i.e. 8th August) shows different results in *CascoViejo* and *Miribilla* (Fig. 8 and 10). Between 8:30 and 11:00 (UTC) ΔT_{mrt} in *Miribilla* varies between -3.6°C and $+2.8^\circ\text{C}$ while in *CascoViejo* values are between -5.9 and -1.2°C .

10.0°C. The results show that the same climate situation (i.e. solar incoming radiation) causes different ΔT_{mrt} values depending on the type of urban development and design. Again the influence of greenery, which has been discussed previously, but also of street design [20,49–51] and urban materials [3,52,53] can modify significantly T_{mrt} . Thus the model needs to be capable to handle precisely the effects of these factors and provide accurate radiation fluxes that on the end condition T_{mrt} estimations.

Additionally, it is interesting to note that during the overcast day (8th August), ΔT_{mrt} in *Casco Viejo* is always negative (Fig. 8). Specific fluctuations as the decrease of $\|\Delta T_{mrt}\|$ values during midday (i.e. sites 4&0) correspond to a reduction in total incoming radiation that is not taken into account by the model. In any case, the underestimation of $T_{mrt_{modelled}}$ can be justified by an underestimation of diffuse $S_{w_{modelled}}$ radiation and urban $L_{w_{modelled}}$ radiation. The influence of the latter is suggested because during the absence of total incoming radiation around sunrise and sunset (i.e. first and last measurements on 8th August, Fig. 8), $T_{mrt_{measured}}$ is still higher than $T_{mrt_{modelled}}$ (i.e. $\Delta T_{mrt}<0$). This result is opposite to the overestimation of $T_{mrt_{modelled}}$ during the clear sky day (7th August) presented previously and reaffirms the conclusion of the inaccuracy of ENVI-met in estimating radiative fluxes as described in Huttner [31].

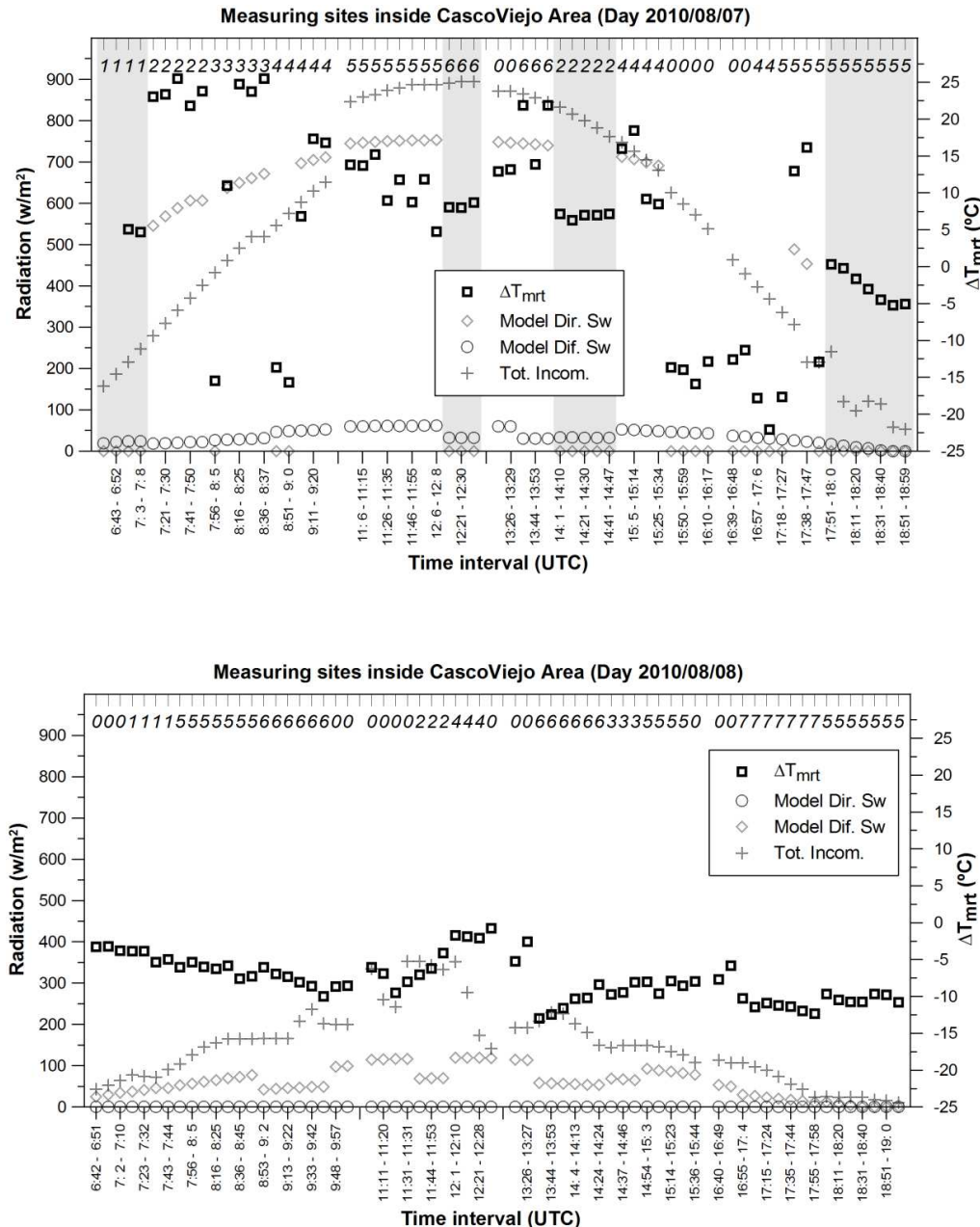


Fig. 8 Temporal evolution in *CascoViejo* of ΔT_{mrt} ($T_{\text{mrt, modelled}} - T_{\text{mrt, measured}}$), measured total incoming radiation (Tot. Incom.) in *Deusto* meteorological station, and modelled direct and diffuse shortwave radiation (Sw). On 2010/08/07, darkened areas represent non-direct sun exposed periods. The rest represent direct sun exposed periods. On 2010/08/08 there is no direct sun exposure due to the overcast situation all day

Finally, the effect of the variability of cloudiness and thus incoming solar radiation along the day can also derive in inaccurate T_{mrt} estimations as is the case of the 6th August (partly covered day). For example, in *Miribilla* (Fig. 9) during the central part of the day ΔT_{mrt} fluctuations are caused by cloud cover variation (e.g. site 2) which is not considered by ENVI-

met since a unique shortwave solar radiation factor can be input for the whole diurnal simulation (see section 3.4)

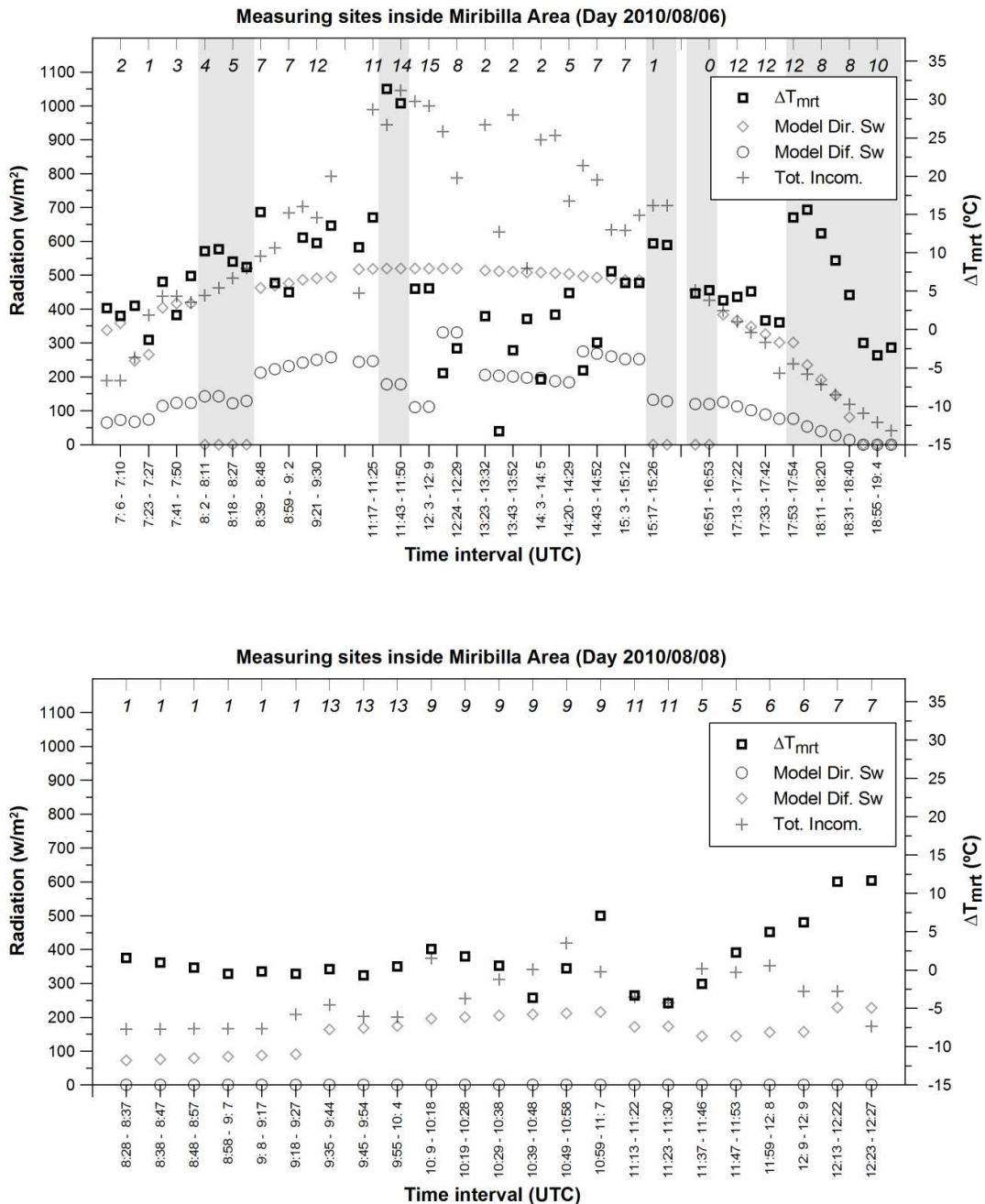


Fig. 9 Temporal evolution in *Miribilla* of ΔT_{mrt} ($T_{mrt\text{modelled}} - T_{mrt\text{measured}}$), measured total incoming radiation (Tot. Incom.) in *Deusto* meteorological station, and modelled direct and diffuse shortwave radiation (Sw). On 2010/08/06, darkened areas represent non-direct sun exposed periods. The rest represent direct sun exposed periods. On 2010/08/08 there is no direct sun exposure due to the overcast situation all day

4.2 Comparison of modelled & field-study PET values

As expected, considering the differences between modelled and measured climate variables described in section 4.1, Pearson's correlation coefficient between $\text{PET}_{\text{fieldstudy}}$ and $\text{PET}_{\text{modelled}}$ including all days and areas is not high ($r=0.73$, $p<0.001$) and RMSE is 5.93°C . It is important to note that these results could differ if other metabolic rate and personal parameters would have been considered for the calculation of PET (see section 3.5).

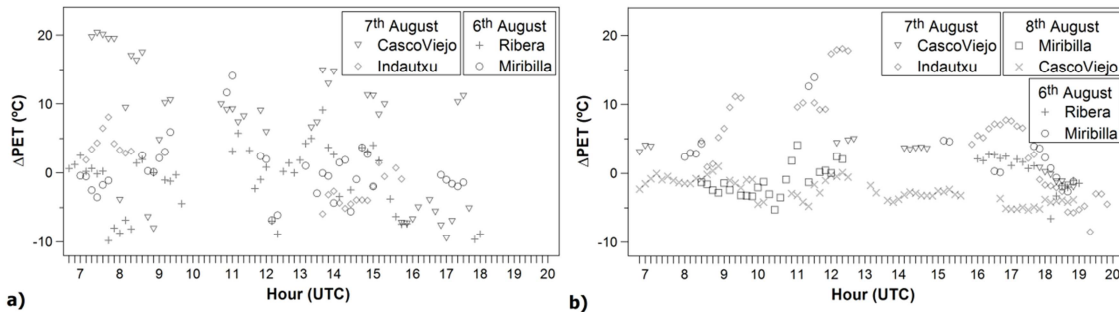


Fig. 10 Temporal evolution of ΔPET ($\text{PET}_{\text{modelled}} - \text{PET}_{\text{fieldstudy}}$) for each area and selected day in a) direct sun exposed site and b) shadow sites and overcast situation (i.e. null direct solar radiation)

Fig. 10 presents the temporal evolution of ΔPET ($\text{PET}_{\text{modelled}} - \text{PET}_{\text{fieldstudy}}$) in direct sun exposed sites and non-direct sun exposed sites (as noted during the field campaigns). Results show low ΔPET values in the case of sites not exposed directly to solar radiation (Fig. 10b). In most of these cases $\text{PET}_{\text{modelled}}$ is slightly underestimated. However, high overestimation of $\text{PET}_{\text{modelled}}$ (i.e. $\Delta\text{PET}>+5^{\circ}\text{C}$) have to be related to the fact that the model is predicting a sun exposed situation (i.e. 6th and 7th August) which in reality is not occurring.

Conversely, in sun exposed sites ΔPET values are much higher (Fig. 10a). Significant $\text{PET}_{\text{modelled}}$ overestimation (i.e. $\Delta\text{PET}>+10^{\circ}\text{C}$) generally corresponds to an overestimation of modelled solar incoming radiation during the morning and afternoon (see section 4.1). Underestimation of $\text{PET}_{\text{modelled}}$ (i.e. $\Delta\text{PET}<-5^{\circ}\text{C}$) again has to be achieved to the model estimating a shadow situation when measurements were made under direct solar radiation.

Based on ΔPET values, it turns out that the evaluation of thermal comfort in urban areas based exclusively on ENVI-met results can include a relevant level of uncertainty. This can also be extended to rural areas. $|\Delta\text{PET}| > 5-6^{\circ}\text{C}$ causes relevant difference in thermal perception [55]. Thus, simulated PET scenarios might lack reality at certain sites. Considering the importance of

Tmrt in PET estimations [19,49,51] as well as the results presented in section 4.3, a reliable estimation of this climate variable becomes crucial for thermal comfort evaluations.

4.3 Analysis of the deviation of PET values

With the aim of explaining Δ PET (for the selected metabolic rate and personal parameters), the relevance of the deviation of each climate variable (i.e. modelled-measured) is evaluated by means of regression analysis. The synthesize results are presented in Table 7 and 8 corresponding to the values of adjusted R squared and the values of standardized regression coefficients (Beta) respectively.

Model	All days and areas	6 th August		7 th August		8 th August	
		Ribera	Miribilla	Indautxu	CascoViejo	Miribilla	CascoViejo
1	0.71*** (ΔTmrt)	0.89*** (ΔTmrt)	0.69*** (ΔTmrt)	0.85*** (ΔTmrt)	0.95*** (ΔTmrt)	0.51*** (ΔWS)	0.54*** (ΔTmrt)
2	0.91*** (ΔTmrt,ΔWS)	0.97*** (ΔTmrt,ΔWS)	0.89*** (ΔTmrt,ΔWS)	0.92*** (ΔTmrt,ΔWS)	0.96** (ΔTmrt,ΔWS)	0.94*** (ΔWS,ΔTmrt)	0.90*** (ΔTmrt,ΔWS)
3	0.92*** (ΔTmrt,ΔWS,ΔTa)	0.99*** (ΔTmrt,ΔWS,ΔRH)	*	0.93** (ΔTmrt,ΔWS,ΔRH)	0.97*** (ΔTmrt,ΔWS,ΔTa)	0.99*** (ΔWS,ΔTmrt,ΔTa)	0.98*** (ΔTmrt,ΔWS,ΔTa)
4	*	*	*	*	*	*	0.98* (ΔTmrt,ΔWS,ΔTa, ΔRH)

*** p<0.001

** p<0.01

* p<0.05

Table 7 Adjusted R² for ΔPET (PET_{modelled} – PET_{fieldstudy}) regression analysis with the independent variables involved.

Independent variable	All days and areas	6 th August		7 th August		8 th August	
		Ribera	Miribilla	Indautxu	CascoViejo	Miribilla	CascoViejo
ΔTmrt	1.01	1.08	0.83	0.82	0.96	0.80	0.79
ΔWS	-0.50	-0.41	-0.44	-0.31	-0.13	-1.13	-0.55
ΔTa	0.10	*	*	*	0.13	0.27	0.45
ΔRH	*	-0.18	*	-0.11	*	*	0.16

Table 8 Standardized regression coefficients (Beta) for ΔPET (PET_{modelled} – PET_{fieldstudy}) regression analysis.

The regression analysis shows that ΔT_{mrt} is the most relevant variable to explain the variations of ΔPET (70.5% of the variance) during the whole measurement period (i.e. including all the days and areas). Similarly correlation of ΔPET with ΔT_{mrt} is significant ($r=0.84$, $p<0.001$).

The results for each individual day and area show that variations in ΔPET can be explained to an important extent by ΔT_{mrt} variations especially during days when direct solar radiation is present (i.e. 6th and 7th August). These days, ΔT_{mrt} can explain between 69.3% and 94.8% of ΔPET variance (Table 7). On the contrary, during the overcast day (8th August), ΔWS also becomes a relevant variable. Specifically, in *Miribilla* ΔWS explains 51.0% of ΔPET variance. In this case, correlation of ΔPET with ΔWS is -0.73 ($p<0.001$), while ΔPET is not significantly correlated with ΔT_{mrt} . In the case of *CascoViejo* on the overcast day, ΔT_{mrt} is the most relevant variable (53.5% of ΔPET variance) and correlation of ΔPET with ΔWS and ΔT_{mrt} is -0.41 ($p<0.001$) and 0.74 ($p<0.001$) respectively. Differences between both areas on overcast conditions are related to the type of urban development. High urban density in *CascoViejo* causes a higher influence of the radiative issue, whereas in more open areas as *Miribilla* WS variability is more relevant.

Results show two different climate patterns for ΔPET variability. On one hand, on partly covered or clear sky days (i.e. 6th and 7th August) ΔT_{mrt} is the most relevant variable. On the other, on overcast days in the absence of direct solar radiation (i.e. 8th August), model estimation of both WS and Tmrt play an important role in ΔPET values. Relevance of ΔRH and ΔTa on ΔPET values are low independently of climate conditions since the $RH_{modelled}$ and $Ta_{modelled}$ are driven by real measured data (see section 4.1).

As expected, statistical results improve significantly when modelled PET is calculated with reliable data (i.e. $PET^*_{modelled}$ is calculated with $Ta_{modelled}$, $RH_{modelled}$, and $Tmrt_{measured}$ and $WS_{measured}$). As shown in Table 9, ΔPET^* ($PET^*_{modelled} - PET_{fieldstudy}$) present important reductions in extreme high and low values. Similarly, relationship between $PET_{fieldstudy}$ and PET of modelled data increase from $r=0.73$ ($p<0.001$) in the case of $PET_{modelled}$ to $r= 0.99$ ($p<0.001$) for $PET^*_{modelled}$.

	$\Delta PET(^{\circ}C)$	$\Delta PET^*(^{\circ}C)$
90 th percentile	9.4	0.5
10 th percentile	-5.2	-2.2
Mean	1.0	-0.7

Table 9 Description of ΔPET ($PET_{modelled} - PET_{fieldstudy}$), ΔPET^* ($PET^*_{modelled} - PET_{fieldstudy}$) values for the whole data available

It turns out that improving the radiation budget solved by ENVI-met and forcing the model with real temporal variations of air flow (i.e. WS and WD) and solar access (i.e. cloudiness) would derive in a better performance of the model, and thus improve PET estimations. Consequently, it is relevant that the actual model limitations should be taken into account and the results provided are used in the adequate context. As presented along section 4, ENVI-met (v4.0) can provide significant deviations in the evaluation of outdoor thermal comfort diurnal cycles.

5. Conclusions

Along the years urban planning and urban design has proven to be a crucial aspect to guarantee suitable thermal comfort levels inside the urban areas and improve quality of life of inhabitants in outdoor spaces. For this aim, adequate tools and methodologies turn to be crucial.

In this study, modelling techniques have been compared with micrometeorological measurements in Bilbao carried out during 3 days covering typical summertime weather conditions (overcast, partly covered and clear sky days).

The evaluation of the performance of ENVI-met model(v4.0) in terms of accuracy has shown that modelled wind speed and mean radiant temperature values present relevant differences with respect to measurements and thus can cause important deviation in thermal comfort estimation. This is due to several reasons:

- On one hand, ENVI-met cannot be forced with precise climate conditions during the simulation period. This is the case of the atmospheric flow characteristics (i.e. wind speed and direction) and the solar radiation adjustment factor that both remain constant along the simulation. The consequence is that the evolution of wind speed and/or mean radiant temperature along the day is not represented correctly by the model, especially

when changing air flow directions occur and/or global radiation (i.e. cloudiness) varies during the diurnal cycle.

- On the other hand, the model presents inaccuracy in the calculation of radiation fluxes that can derive in relevant deviation of mean radiant temperature estimations. It is especially important the overestimation of incoming solar radiation during the morning and afternoon, but errors have also been found in the other components of the radiation budget solved by the model (i.e. diffuse/reflected shortwave and longwave radiation).
- Finally, the model spatial resolution can in certain cases be a limitation for a detailed definition of the morphological aspect of urban elements and thus their influence in climate variables (e.g. solar radiation exposure)

In the use of ENVI-met during this study, it has been proved that during clear sky days mean radiant temperature deviation (i.e. difference between modelled and measured values) is the most relevant aspect influencing deviation of PET values, while on overcast days in the absence of direct solar radiation, model estimation of both wind speed and mean radiant temperature play an important role in PET deviation.

The results presented in this paper have shown that in the evaluation of the diurnal cycle of thermal comfort levels in urban areas, ENVI-met model can provide relevant deviations with respect to measurements. Similar conclusions are expected for non-urban areas. Thus, despite ENVI-met is a commonly used model that can provide in certain cases useful information (e.g. comparison of urban planning scenarios during typical meteorological conditions), it is important that users are aware of the limitations of the model and the accuracy of the results.

6. Acknowledgements

The authors would like to acknowledge Dipl. German Fernandez for the help with the measuring devices and Dipl. Jon Arrizabalaga and Dipl. Lexuri Yurrebaso for the help during the measurement campaigns. Climatic data was provided by the Environmental Department and the Basque Meteorological Agency in the Basque Country (Spain). The work leading to these results has received funding from: a) the Basque Government's ETORTEK programme within the framework of the Basque Science, Technology and Innovation Plan 2010 under the Project K-Egokitzen (2007-2011), and b) the European Community's Seventh Framework Programme under Grant Agreement No. 308497, Project RAMSES - Reconciling Adaptation, Mitigation and Sustainable Development for Cities (2012-2016).

7. References

- [1] Oliveira S, Andrade H, Vaz T. The cooling effect of green spaces as a contribution to the mitigation of urban heat: A case study in Lisbon. *Build Environ* 2011;46:2186–94. doi:10.1016/j.buildenv.2011.04.034.
- [2] Ng E, Chen L, Wang Y, Yuan C. A study on the cooling effects of greening in a high-density city: An experience from Hong Kong. *Build Environ* 2012;47:256–71. doi:10.1016/j.buildenv.2011.07.014.
- [3] Doulos L, Santamouris M, Livada I. Passive cooling of outdoor urban spaces. The role of materials. *Sol Energy* 2004;77:231–49. doi:10.1016/j.solener.2004.04.005.
- [4] Carnielo E, Zinzi M. Optical and thermal characterisation of cool asphalts to mitigate urban temperatures and building cooling demand. *Build Environ* 2013;60:56–65. doi:10.1016/j.buildenv.2012.11.004.
- [5] Oke TR. *Boundary Layer Climates*. New York: Routledge; 1987.
- [6] Boumans RJM, Phillips DL, Victery W, Fontaine TD. Developing a model for effects of climate change on human health and health–environment interactions: Heat stress in Austin, Texas. *Urban Clim* 2014;8:78–99. doi:10.1016/j.uclim.2014.03.001.
- [7] Luber G, McGeehin M. Climate Change and Extreme Heat Events. *Am J Prev Med* 2008;35:429–35. doi:10.1016/j.amepre.2008.08.021.
- [8] Nikolopoulou M, Lykoudis S. Thermal comfort in outdoor urban spaces: Analysis across different European countries. *Build Environ* 2006;41:1455–70. doi:10.1016/j.buildenv.2005.05.031.
- [9] Ren C, Ng EY, Katzschner L. Urban climatic map studies: a review. *Int J Climatol* 2011;31:2213–33. doi:10.1002/joc.2237.
- [10] Acero JA, Arrizabalaga J, Kupski S, Katzschner L. Deriving an Urban Climate Map in coastal areas with complex terrain in the Basque Country (Spain). *Urban Clim* 2013;4:35–60. doi:10.1016/j.uclim.2013.02.002.
- [11] Nikolopoulou M, Lykoudis S. Use of outdoor spaces and microclimate in a Mediterranean urban area. *Build Environ* 2007;42:3691–707. doi:10.1016/j.buildenv.2006.09.008.
- [12] Mayer H. Urban bioclimatology. *Experientia* 1993;49:957–63. doi:10.1007/BF02125642.
- [13] VDI. Methods for the human-biometeorological assessment of climate and air hygiene for urban and regional planning - Part I: Climte. Beuth, Berlin: 1998.
- [14] Parsons K. Human thermal environments: the effect of hot, moderate, and cold environments on human health, comfort and performance. London, New York: Taylor & Francis; 2003.

- [15] Matzarakis A, Mayer H, Iziomon MG. Applications of a universal thermal index: physiological equivalent temperature. *Int J Biometeorol* 1999;43:76–84. doi:10.1007/s004840050119.
- [16] Mayer H, Höppe P. Thermal comfort of man in different urban environments. *Theor Appl Climatol* 1987;38:43–9. doi:10.1007/BF00866252.
- [17] Holst J, Mayer H. Impacts of street design parameters on human-biometeorological variables. *Meteorol Zeitschrift* 2011;20:541–52. doi:<http://dx.doi.org/10.1127/0941-2948/2011/0254>.
- [18] Ali-Toudert F, Mayer H. Thermal comfort in an east-west oriented street canyon in Freiburg (Germany) under hot summer conditions. *Theor Appl Climatol* 2007;87:223–37. doi:10.1007/s00704-005-0194-4.
- [19] Mayer H, Holst J, Dostal P, Imbery F, Schindler D. Human thermal comfort in summer within an urban street canyon in Central Europe. *Meteorol Zeitschrift* 2008;17:241–50. doi:10.1127/0941-2948/2008/0285.
- [20] Ali-Toudert F, Mayer H. Effects of asymmetry, galleries, overhanging façades and vegetation on thermal comfort in urban street canyons. *Sol Energy* 2007;81:742–54. doi:10.1016/j.solener.2006.10.007.
- [21] Müller N, Kuttler W, Barlag A-B. Counteracting urban climate change: adaptation measures and their effect on thermal comfort. *Theor Appl Climatol* 2013;115:243–57. doi:10.1007/s00704-013-0890-4.
- [22] Ketterer C, Matzarakis A. Human-biometeorological assessment of heat stress reduction by replanning measures in Stuttgart, Germany. *Landsc Urban Plan* 2014;122:78–88. doi:10.1016/j.landurbplan.2013.11.003.
- [23] Gulyás Á, Unger J, Matzarakis A. Assessment of the microclimatic and human comfort conditions in a complex urban environment: Modelling and measurements. *Build Environ* 2006;41:1713–22. doi:10.1016/j.buildenv.2005.07.001.
- [24] Bruse M, Fleer H. Simulating surface-plant-air interactions inside urban environments with a three dimensional numerical model. *Environ Model Softw* 1998;13:373–84. doi:10.1016/S1364-8152(98)00042-5.
- [25] Bruse M. ENVI-met 4 2014. <http://www.envi-met.info>.
- [26] Matzarakis A, Rutz F, Mayer H. Modelling radiation fluxes in simple and complex environments--application of the RayMan model. *Int J Biometeorol* 2007;51:323–34. doi:10.1007/s00484-006-0061-8.
- [27] Lindberg F, Holmer B, Thorsson S. SOLWEIG 1.0 - Modelling spatial variations of 3D radiant fluxes and mean radiant temperature in complex urban settings. *Int J Biometeorol* 2008;52:697–713. doi:10.1007/s00484-008-0162-7.
- [28] Chow WTL, Pope RL, Martin CA, Brazel AJ. Observing and modeling the nocturnal park cool island of an arid city: Horizontal and vertical impacts. *Theor Appl Climatol* 2011;103:197–211. doi:10.1007/s00704-010-0293-8.

- [29] Ketterer C, Matzarakis A. Comparison of different methods for the assessment of the urban heat island in Stuttgart, Germany. *Int J Biometeorol* 2014. doi:10.1007/s00484-014-0940-3.
- [30] Krüger EL, Minella FO, Rasia F. Impact of urban geometry on outdoor thermal comfort and air quality from field measurements in Curitiba, Brazil. *Build Environ* 2011;46:621–34. doi:10.1016/j.buildenv.2010.09.006.
- [31] Huttner S. Further development and application of the 3D microclimate simulation ENVI-met. University of Mainz, 2012.
- [32] Yang X, Zhao L, Bruse M, Meng Q. Evaluation of a microclimate model for predicting the thermal behavior of different ground surfaces. *Build Environ* 2013;60:93–104. doi:10.1016/j.buildenv.2012.11.008.
- [33] Acero JA, Arrizabalaga J, Kupski S, Katzschner L. Urban heat island in a coastal urban area in northern Spain. *Theor Appl Climatol* 2012;113:137–54. doi:10.1007/s00704-012-0774-z.
- [34] González-Aparicio I, Hidalgo J. Dynamically based future daily and seasonal temperature scenarios analysis for the northern Iberian Peninsula. *Int J Climatol* 2012;32:1825–33. doi:10.1002/joc.2397.
- [35] Euskalmet - Basque Meteorological Agency. Climate variables analysis: cloud cover n.d. http://www.euskalmet.euskadi.net/s07-5853x/es/contenidos/informacion/ana_cobertura/es_7271/es_cobertura.html.
- [36] Millán MM, Otamendi E, Alonso LA, Ureta I. Experimental Characterization of Atmospheric Diffusion in Complex Terrain with Land-Sea Interactions. *JAPCA* 1987;37:807–11. doi:10.1080/08940630.1987.10466271.
- [37] Thorsson S, Lindberg F, Eliasson I, Holmer B. Different methods for estimating the mean radiant temperature in an outdoor urban setting. *Int. J. Climatol.*, vol. 27, 2007, p. 1983–93. doi:10.1002/joc.1537.
- [38] Dear R De. Png-pong globe thermometers for mean radiant temperatures. *Heat Vent Eng J Air Cond* 1987;60:10–1.
- [39] Davenport A. Rationale for determining design wind velocities. *Amer Soc Civ Eng Struct Div J* 1960;86:39–68.
- [40] Höppe P. The physiological equivalent temperature - a universal index for the biometeorological assessment of the thermal environment. *Int J Biometeorol* 1999;43:71–5. doi:10.1007/s004840050118.
- [41] Steeneveld GJ, Koopmans S, Heusinkveld BG, Theeuwes NE. Landscape and Urban Planning Refreshing the role of open water surfaces on mitigating the maximum urban heat island effect. *Landsc Urban Plan* 2014;121:92–6. doi:10.1016/j.landurbplan.2013.09.001.
- [42] Theeuwes NE, Solcerova A, Steeneveld GL. Modeling the influence of open water surfaces on the summertime temperature and thermal comfort in the city. *J Geophys Res Atmos* 2013;118:8881–96. doi:10.1002/jgrd.50704.

- [43] Bowler DE, Buyung-Ali L, Knight TM, Pullin AS. Urban greening to cool towns and cities: A systematic review of the empirical evidence. *Landsc Urban Plan* 2010;97:147–55. doi:10.1016/j.landurbplan.2010.05.006.
- [44] Yan H, Wang X, Hao P, Dong L. Study on the microclimatic characteristics and human comfort of park plant communities in summer. *Procedia Environ Sci* 2012;13:755–65. doi:10.1016/j.proenv.2012.01.069.
- [45] Cui L, Shi J. Urbanization and its environmental effects in Shanghai, China. *Urban Clim* 2012;2:1–15. doi:10.1016/j.uclim.2012.10.008.
- [46] Ng E. Policies and technical guidelines for urban planning of high-density cities - air ventilation assessment (AVA) of Hong Kong. *Build Environ* 2009;44:1478–88. doi:10.1016/j.buildenv.2008.06.013.
- [47] Lopes A, Lopes S, Matzarakis A, Alcoforado MJ. The influence of the summer sea breeze on thermal comfort in funchal (Madeira). A contribution to tourism and urban planning. *Meteorol Zeitschrift* 2011;20:553–64. doi:10.1127/0941-2948/2011/0248.
- [48] Song B, Park K, Jung S. Validation of ENVI-met Model with In Situ Measurements Considering Spatial Characteristics of Land Use Types. *J Korean Assoc Geog Inf Stud* 2014;17:156–72.
- [49] Taleghani M, Kleerekoper L, Tenpierik M, van den Dobbelenstein A. Outdoor thermal comfort within five different urban forms in the Netherlands. *Build Environ* 2014;83:65–78. doi:10.1016/j.buildenv.2014.03.014.
- [50] Givoni B. Climate consideration in building and urban design. Wiley; 1998.
- [51] Herrmann J, Matzarakis A. Mean radiant temperature in idealised urban canyons - example from Freiburg, Germany. *Int J Biometeorol* 2012;56:199–203.
- [52] Erell E, Pearlmutter D, Boneh D, Kutiel PB. Effect of high-albedo materials on pedestrian heat stress in urban street canyons. *Urban Clim* 2014;10:367–86. doi:10.1016/j.uclim.2013.10.005.
- [53] Georgakis C, Zoras S, Santamouris M. Studying the effect of “cool” coatings in street urban canyons and its potential as a heat island mitigation technique. *Sustain Cities Soc* 2014;13:20–31. doi:10.1016/j.scs.2014.04.002.
- [54] Willmott C. Some comments on the evaluation of model performance. *B Am Meteorol Soc* 1982;63:1309–69.
- [55] Matzarakis A, Mayer H. Another kind of environmental stress: thermal stress. *WHO Newsl* 1996;7–10.

Highlights

- ENVI-met can lack accuracy in Tmrt and WS estimations
- Differences between measured and modelled thermal comfort levels can be relevant
- Knowing limitations of models used for thermal comfort evaluation is essential